Two lasing thresholds in semiconductor lasers with a quantum-confined active region

Levon V. Asryan[a)]
State University of New York at Stony Brook, Stony Brook, New York 11794-2350 and Ioffe Physico-Technical Institute, St. Petersburg 194021, Russia

Serge Luryi[b)]
State University of New York at Stony Brook, Stony Brook, New York 11794-2350

(Received 22 July 2003; accepted 30 October 2003)

We show that the free-carrier-density dependence of internal optical loss gives rise, in general, to the existence of a second lasing threshold above the conventional threshold. Above the second threshold, the light-current characteristic is two-valued up to a maximum current at which the lasing is quenched. © *2003 American Institute of Physics.* [DOI: 10.1063/1.1636245]

Internal optical loss adversely affects operating characteristics of semiconductor lasers. Because of the lower value of the optical confinement factor, the effect of internal loss is stronger for lasers with a reduced-dimensionality active region, such as quantum well (QW), quantum wire (QWR), and quantum dot (QD) lasers, than for bulk lasers.[1]

All different processes contributing to the internal loss can be grouped into two categories: one, such as free-carrier absorption in the optical confinement layer (OCL), or simply waveguide, dependent on the injection carrier density; the other, such as interface scattering or absorption in the cladding layers, insensitive to this density. Absorption in the active region of QW and QWR lasers is relatively small compared to absorption in the OCL, at least at high injection currents j [or high temperatures T (see Refs. 2 and 3)]. The analogous process in the active region of QD lasers—which is carrier photoexcitation from the discrete levels to the continuous-spectrum states—is also small.[4,5] Neglecting these processes, we must be concerned only with the free-carrier density n in the OCL. Therefore, we need a relation between n and the occupancy of states in the quantum-confined active region, involved in the lasing transition. At sufficiently high temperatures and below the lasing threshold, this relation is given by equilibrium statistics and is of the form[4]

$$n=n_1\frac{f_n}{1-f_n}, \tag{1}$$

where $n_1=N_c^{\mathrm{OCl}}\exp(-E_n/T)$, $N_c^{\mathrm{OCL}}=2(m_c^{\mathrm{OCL}}T/2\pi\hbar^2)^{3/2}$, E_n is the carrier excitation energy from a reduced-dimensionality active region, and the temperature T is measured in units of energy. The function f_n is the Fermi–Dirac distribution, describing the occupancy of the confined states. For QW or QWR lasers, f_n is the occupancy of the subband-edge level, involved into the lasing transitions. For a QD laser, f_n is the occupancy of the discrete level.

Assuming equal electron and hole occupancies ($f_n=f_p$), and writing the total net internal loss coefficient α_{int} (the quantity we shall refer to simply as the internal loss) as the sum of a constant α_0 and a component linear in n, the lasing threshold condition is brought into the form

$$g^{\max}(2f_n-1)=\beta+\alpha_0+\sigma_{\mathrm{int}}n_1\frac{f_n}{1-f_n}, \tag{2}$$

where $g^{\max}$ is the maximum (saturation) value of the modal gain $g(f_n)=g^{\max}(2f_n-1)$, β is the mirror loss, and $\sigma_{\mathrm{int}}=\mathrm{const}(n)$ can be viewed as an effective cross section for all absorption loss processes (for the type of carrier that dominates absorption).

The solutions of Eq. (2) are [Fig. 1(a)]

$$f_{n1,n2}=f_n^{\mathrm{crit}}\mp\sqrt{(f_n^{\mathrm{crit}})^2-f_{n0}-\frac{1}{2}\frac{\alpha_0}{g^{\max}}}, \tag{3}$$

where

$$f_n^{\mathrm{crit}}=\frac{1}{2}\left(1+f_{n0}+\frac{1}{2}\frac{\alpha_0}{g^{\max}}-\frac{1}{2}\frac{\sigma_{\mathrm{int}}n_1}{g^{\max}}\right) \tag{4}$$

is the "critical" solution {when the cavity length equals its minimum tolerable value [see Eq. (13)]}, and

$$f_{n0}=\frac{1}{2}\left(1+\frac{\beta}{g^{\max}}\right) \tag{5}$$

is the solution in the absence of internal loss.

Both solutions (3) are physically meaningful and describe two distinct lasing thresholds. The lower solution (f_{n1}) is the conventional threshold, similar to f_{n0} but modified by α_{int} The second solution (f_{n2}) appears purely as a consequence of the carrier-density-dependent α_{int} in the OCL.

In the absence of lasing, the injection current density has the following relation to f_n:[4,6]

$$j=j_{\mathrm{spon}}^{\mathrm{active}}(f_n)+ebBn_1^2\frac{f_n^2}{(1-f_n)^2}, \tag{6}$$

[a)]Electronic mail: asryan@ece.sunysb.edu; URL: http://www.ioffe.rssi.ru/Dep_TM/asryan.html
[b)]Electronic mail: Serge.Luryi@sunysb.edu; URL: http://www.ece.sunysb.edu/~serge

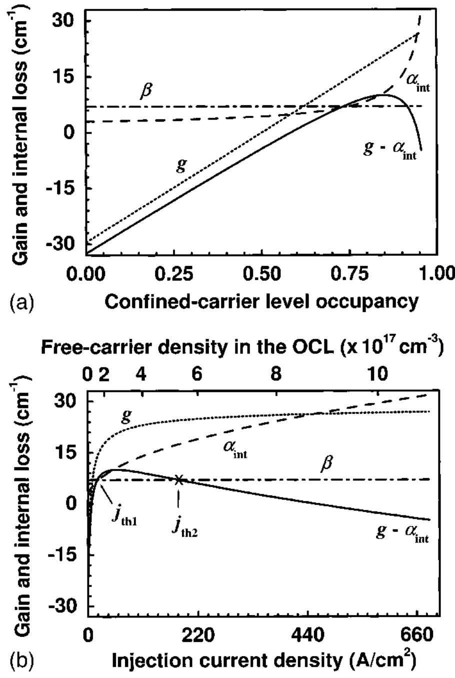

FIG. 1. Illustration of the threshold condition (2) and the two lasing thresholds. Modal gain $g=g^{\max}(2f_n-1)$ [inclined dotted line in (a) and dotted curve in (b)], internal loss $\alpha_{\rm int}=\alpha_0+\sigma_{\rm int}n=\alpha_0+\sigma_{\rm int}n_1 f_n/(1-f_n)$ (dashed curve) and difference of modal gain and internal loss (solid curve) against confined-carrier-level occupancy in the active region f_n (a), free-carrier density in the OCL n [(b), top axis] and injection current density j [(b), bottom axis]. The intersections of the solid curve and the horizontal dash-dotted line for the mirror loss $\beta=(1/L)\ln(1/R)$ are the solutions (3) of (2). A GaInAsP/InP-based QD-heterostructure lasing near 1.55 μm (see Refs. 4–6) is considered for illustration. We assume 10% QD size fluctuations and $N_S=6.11\times10^{10}$ cm^{-2}; at these parameters, $g^{\max}=29.52$ cm^{-1}. At $T=300$ K, $n_1=5.07\times10^{16}$ cm^{-3}. The mirror loss $\beta=7$ cm^{-1}. α_0 and $\sigma_{\rm int}$ are plausibly taken to be 3 cm^{-1} and 2.67×10^{-17} cm^{-1}, respectively.

where b is the OCL thickness and B is the radiative constant for the OCL.

Next, we need a relation between the spontaneous recombination current density $j_{\rm spon}^{\rm active}$ and the occupancy f_n. For QW, QWR, and QD lasers, we have, respectively,[4,6]

$$j_{\rm spon}^{\rm QW}=eN_{\rm QW}B_{\rm 2D}n_{\rm 2D}^2(f_n), \tag{7}$$

where $N_{\rm QW}$ is the number of QWs and $B_{\rm 2D}$ is the radiative constant for a two-dimensional (2D) region (in cm^2/s);

$$j_{\rm spon}^{\rm QWR}=eN_L B_{\rm 1D}n_{\rm 1D}^2(f_n), \tag{8}$$

where N_L is the linear density of QWRs and $B_{\rm 1D}$ is the radiative constant for a one-dimensional region (in cm/s); and

$$j_{\rm spon}^{\rm QD}=\frac{eN_S}{\tau_{\rm QD}}f_n^2, \tag{9}$$

where N_S is the surface density of QDs and $\tau_{\rm QD}$ is the radiative lifetime in a QD.

The 2D-carrier density $n_{\rm 2D}$ in a QW is expressed in terms of f_n as follows:[7]

$$n_{\rm 2D}=N_c^{\rm 2D}\ln\frac{1}{1-f_n}, \tag{10}$$

where $N_c^{\rm 2D}=m_c^{\rm QW}T/\pi\hbar^2$. A functional relationship between $n_{\rm 1D}$ in a QWR and f_n is also readily calculated, albeit not as a closed-form expression.

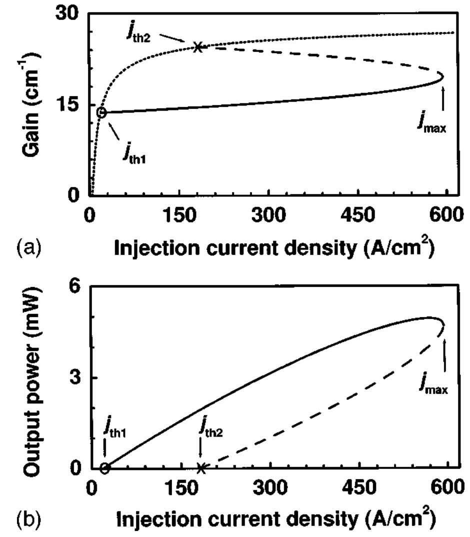

FIG. 2. Two-valued characteristics: gain-current (a) and light-current (b). The branches corresponding to the lower and the upper lasing regimes (solid and dashed curves, respectively) merge together at the point $j_{\max}$ which defines the maximum operating current. At $j>j_{\max}$, the lasing is quenched. The dotted curve in (a) is the gain-current dependence for a nonlasing regime; the intersection of the solid (dashed) curve and the dotted curve determines $j_{\rm th1}(j_{\rm th2})$. In (b), the assumed stripe width $w=2\,\mu$m.

The lower and the upper threshold current densities ($j_{\rm th1}$ and $j_{\rm th2}$) are given by Eq. (6), wherein one substitutes either $f_n=f_{n1}$ or $f_n=f_{n2}$.

The existence of a second lasing threshold stems from the nonmonotonic dependence of $g-\alpha_{\rm int}$ on f_n [Fig. 1(a)] or, equivalently, on n or j [Fig. 1(b)]. The point is that the modal gain $g(f_n)$ increases linearly with f_n [Fig. 1(a)] and saturates at its maximum value $g^{\max}$ as $f_n\rightarrow1$ {which corresponds to $n\rightarrow\infty$ and $j\rightarrow\infty$ [see Eqs. (1) and (6), and Fig. 1(b)]}. At the same time, $\alpha_{\rm int}$ is superlinear in f_n [see Eq. (2) and Fig. 1(a)] and increases infinitely as $f_n\rightarrow1$. At a certain f_n (i.e., at a certain j), the rate of increase in $\alpha_{\rm int}$ with j will inevitably equal that of increase in g, and hence the difference $g-\alpha_{\rm int}$ will peak. Any further increase of j will decrease the difference $g-\alpha_{\rm int}$ [cf. Fig. 1(b)]. This corresponds to the so-called "loss-multiplication" regime, discussed in Refs. 2 and 3 for QW lasers (and attributed to the pile-up of carriers due to electrostatic band-profile deformation[8,9]) and in Refs. 10 and 11 for QD lasers. As evident from our analysis, this regime and the second lasing threshold are inherent to all structures in which $\alpha_{\rm int}$ depends on n.

It should be noted that the second lasing threshold can also arise due to other mechanisms; for example, carrier heating. As the carrier temperature increases with j,[9,12–15] the modal gain itself can become a nonmonotonic function of j, decreasing at high j.[13]

In a continuous-wave (CW) operation, increasing j from zero, one reaches the first lasing threshold $j_{\rm th1}$. Above this threshold, the difference between the gain and the internal loss is pinned at the value of the mirror loss β and hence, Fig. 1 (which is valid for determining the positions of both thresholds) no longer applies. What actually happens above $j_{\rm th1}$ is shown in Fig. 2, derived by rigorously solving the rate equations in the presence of light generation.

Above the second threshold $j_{\rm th2}$ and up to a maximum

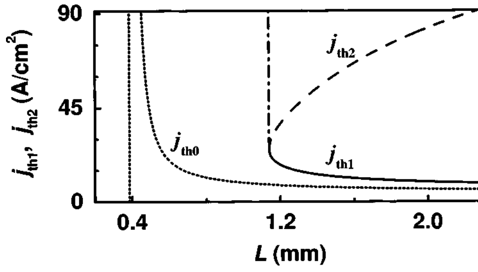

FIG. 3. The lower and the upper threshold current densities j_{th1} and j_{th2} (solid and dashed curves, respectively) against L. The curve for j_{th1} join smoothly the vertical dash-dotted line at the critical point. The dotted curve and the vertical dotted line show the threshold current density j_{th0} and its asymptote at the critical point in the absence of internal loss.

current j_{max}, both the gain-current dependence [Fig. 2(a)] and the light-current characteristic [Fig. 2(b)] are two-valued. At $j=j_{max}$, the two branches merge in both characteristics. The origin of this striking behavior is clear. As α_{int} increases with the current, the gain strictly follows it so as to maintain the stable generation condition $g-\alpha_{int}=\beta$. This continues up to the maximum pump current j_{max} at which the lasing is quenched.

At this time, we cannot propose a definite experimental technique to access the lower branch of the light-current characteristic [Fig. 2(b)]. Analysis of the stability of the lower-branch regime will be published elsewhere. Nevertheless, we stress that an experimental determination of the second threshold would provide us with a new and valuable technique for measuring the loss parameters. Indeed, with the measured j_{th1} and j_{th2}, the values of f_{n1} and f_{n2} can be calculated from Eq. (6). α_0 and σ_{int} can then be expressed in terms of f_{n1} and f_{n2} as follows [see Eqs. (3) and (4)]:

$$\alpha_0=2g^{max}(f_{n1}f_{n2}-f_{n0}), \tag{11}$$

$$\sigma_{int}=2\frac{g^{max}}{n_1}(1+f_{n1}f_{n2}-f_{n1}-f_{n2}). \tag{12}$$

When only one threshold exists, the carrier-density-dependent internal loss is negligible and α_0 is determined from the "$-$" solution in Eq. (3).

The thresholds j_{th1} and j_{th2} depend on the cavity length L (Fig. 3) and approach each other as L decreases. At a certain critical L that we shall call the minimum tolerable cavity length L^{min}, the horizontal line for the mirror loss β is tangent to the curve for $g-\alpha_{int}$ at its maximum (Fig. 1). In this case, the threshold condition has only one solution, $f_{n1}=f_{n2}=f_n^{crit}$, and $j_{th1}=j_{th2}$. For $L<L^{min}$, there is no solution of the threshold condition and hence no lasing is possible. The equation for L^{min} is

$$L^{min}=\frac{L_0^{min}}{\left(\sqrt{2}-\sqrt{\frac{\sigma_{int}n_1}{g^{max}}}\right)^2-1-\frac{\alpha_0}{g^{max}}}, \tag{13}$$

where $L_0^{min}=(1/g^{max})\ln(1/R)$ is the minimum cavity length in the absence of α_{int} (see Ref. 16 for L_0^{min} for a QD laser), and R is the mirror reflectivity. In Eq. (4), $\beta^{max}=(1/L^{min})\ln(1/R)$ should be entered for β in this case.

Measurement of L^{min} provide yet another way of the internal loss parameters determination. For example, L^{min} can be measured for two structures characterized by different mirror reflectivities. With these two values of L^{min}, Eq. (13) will give a set of two equations in α_0 and σ_{int} (provided the other parameters are fixed).

The restriction L^{min} can be considerably more stringent compared to L_0^{min}. Thus, for a QD laser similar to that considered in Refs. 4–6 (see the caption to Fig. 1 for the parameters), at $\alpha_0=3$ cm^{-1} and $\sigma_{int}=2.67\times10^{-17}$ cm^{-1}, the maximum tolerable mirror loss is $\beta^{max}=10$ cm^{-1}. Assuming as-cleaved facet reflectivity at both ends ($R=0.32$), this yields $L^{min}=1.139$ mm, which is almost a threefold increase compared to $L_0^{min}=386$ μm. Hence, the absence of lasing often observed in short-cavity QD structures can be attributed to internal loss, which is consistent with the discussion in Refs. 10 and 11.

All equations of this paper apply equally to QW, QWR, and QD lasers. One specifies the type of laser by substituting the relevant expression for g^{max} and the appropriate relation between j_{spon}^{active} and f_n [see Eqs. (6)–(9)].

In conclusion, we predict the existence of a second (upper) lasing threshold when the internal loss has a component that increases with the carrier density in the waveguide. Any measurement of the upper threshold contains valuable information about the internal loss parameters. These parameters are not easy to measure directly and our theory may yield a new experimental method.

This work was supported in part by the AFOSR MURI under Grant F49620-00-1-0331 and the New York State Center for Advanced Sensor Technology. The work of L.V.A. was also supported by the RFBR and by the Russian Program "Physics of Solid State Nanostructures."

[1] G. P. Agrawal and N. K. Dutta, *Long-Wavelength Semiconductor Lasers* (Van Nostrand Reinhold, New York, 1986).
[2] S. Seki, H. Oohasi, H. Sugiura, T. Hirono, and K. Yokoyama, Appl. Phys. Lett. **67**, 1054 (1995).
[3] S. Seki, H. Oohasi, H. Sugiura, T. Hirono, and K. Yokoyama, J. Appl. Phys. **79**, 2192 (1996).
[4] L. V. Asryan and R. A. Suris, Semicond. Sci. Technol. **11**, 554 (1996).
[5] L. V. Asryan and R. A. Suris, Semiconductors **35**, 343 (2001).
[6] L. V. Asryan, S. Luryi, and R. A. Suris, IEEE J. Quantum Electron. **39**, 404 (2003).
[7] K. J. Vahala and C. E. Zah, Appl. Phys. Lett. **52**, 1945 (1988).
[8] S. Seki and K. Yokoyama, J. Appl. Phys. **77**, 5180 (1995).
[9] L. V. Asryan, N. A. Gun'ko, A. S. Polkovnikov, G. G. Zegrya, R. A. Suris, P.-K. Lau, and T. Makino, Semicond. Sci. Technol. **15**, 1131 (2000).
[10] A. E. Zhukov, A. R. Kovsh, V. M. Ustinov, and Zh. I. Alferov, Laser Phys. **13**, 319 (2003).
[11] A. R. Kovsh, N. A. Maleev, A. E. Zhukov, S. S. Mikhrin, A. P. Vasil'ev, E. A. Semenova, Yu. M. Shernyakov, M. V. Maximov, D. A. Livshits, V. M. Ustinov, N. N. Ledentsov, D. Bimberg, and Zh. I. Alferov, J. Cryst. Growth **251**, 729 (2003).
[12] P. G. Eliseev, *Introduction to the Physics of Injection Lasers* (Nauka, Moscow, 1983) (in Russian).
[13] V. B. Gorfinkel, S. Luryi, and B. Gelmont, IEEE J. Quantum Electron. **32**, 1995 (1996).
[14] V. Gorfinkel, M. Kisin, and S. Luryi, Opt. Express **2**, 125 (1998).
[15] L. V. Asryan, N. A. Gun'ko, A. S. Polkovnikov, R. A. Suris, G. G. Zegrya, B. B. Elenkrig, S. Smetona, J. G. Simmons, P.-K. Lau, and T. Makino, Semicond. Sci. Technol. **14**, 1069 (1999).
[16] L. V. Asryan and R. A. Suris, IEEE J. Quantum Electron. **36**, 1151 (2000).